Temperature fluctuation of the Iceland mantle plume through time

AGU PUBLICATIONS

Geochemistry, Geophysics, Geosystems

RESEARCH ARTICLE
10.1002/2015GC006059

Temperature fluctuation of the Iceland mantle plume through time

Holly E. Spice[1,2], J. Godfrey Fitton[1], and Linda A. Kirstein[1]

[1]School of GeoSciences, University of Edinburgh, Edinburgh, UK, [2]Scottish Universities Physics Alliance, Centre for Science at Extreme Conditions, School of Physics and Astronomy, University of Edinburgh, Edinburgh, UK

Key Points:
- Temperature of the Iceland mantle plume through time using Al-in-olivine thermometry
- The T anomaly at ~61 Ma was uniform across an area of 2000 km in diameter
- The plume T has fluctuated on a 10^7 year time scale and is currently increasing

Supporting Information:
- Supporting Information S1
- Data Set S1
- Data Set S2

Correspondence to:
H. E. Spice,
holly.spice@ed.ac.uk

Citation:
Spice, H. E., J. G. Fitton, and L. A. Kirstein (2016), Temperature fluctuation of the Iceland mantle plume through time, *Geochem. Geophys. Geosyst.*, *17*, doi:10.1002/2015GC006059.

Received 11 AUG 2015
Accepted 5 JAN 2016
Accepted article online 8 JAN 2016

Abstract The newly developed Al-in-olivine geothermometer was used to find the olivine-Cr-spinel crystallization temperatures of a suite of picrites spanning the spatial and temporal extent of the North Atlantic Igneous Province (NAIP), which is widely considered to be the result of a deep-seated mantle plume. Our data confirm that start-up plumes are associated with a pulse of anomalously hot mantle over a large spatial area before becoming focused into a narrow upwelling. We find that the thermal anomaly on both sides of the province at Baffin Island/West Greenland and the British Isles at ~61 Ma across an area ~2000 km in diameter was uniform, with Al-in-olivine temperatures up to ~300°C above that of average mid-ocean ridge basalt (MORB) primitive magma. Furthermore, by combining our results with geochemical data and existing geophysical and bathymetric observations, we present compelling evidence for long-term (>10^7 year) fluctuations in the temperature of the Iceland mantle plume. We show that the plume temperature fell from its initial high value during the start-up phase to a minimum at about 35 Ma, and that the mantle temperature beneath Iceland is currently increasing.

1. Introduction

Mantle plumes are buoyancy-driven flows originating from deep within the Earth and result in large mantle thermal anomalies. Large igneous province (LIP) volcanism is commonly considered to be the surface expression of deep mantle plumes. Voluminous magma generation over a large spatial area is associated with the early plume-head stage of activity and, with time, melting becomes focused into a narrow mantle upwelling in the plume tail. The magmatic productivity of plumes varies with time, and a key question concerns whether this reflects variation in plume temperature or mantle fertility. The North Atlantic Igneous Province (NAIP) is one of the best studied LIPs on Earth, and it is generally accepted to be the result of a deep-seated mantle plume that presently underlies Iceland. Iceland is the only part of the NAIP (Figure 1) that remains active, and it represents the subaerial expression of an extensive basalt plateau formed as the result of the interaction of the mantle plume and the Mid-Atlantic spreading axis. However, some authors have argued that a mantle plume is not required to produce the enhanced melting beneath Iceland [*Foulger and Anderson*, 2005; *Foulger et al.*, 2005] and so a key objective of this work is to test objectively the hypothesis that a thermal plume was responsible for the NAIP and to place quantitative constraints on its magnitude.

The North Atlantic region provides a unique insight into the temporal evolution of a mantle plume and its continuous, but variable, record of mantle melting from its initial impact on the lithosphere at 61 Ma to the present time [*Saunders et al.*, 1997]. Bathymetric and geophysical studies indicate that the mantle plume underlying Iceland has been subject to fluctuations in melt production over variable time scales. Prominent topographic and gravity V-shaped ridges (VSRs) either side of the Reykjanes Ridge south of Iceland are the result of fluctuating magma production [*Vogt*, 1971; *White et al.*, 1995; *Jones et al.*, 2002]. It is now widely accepted that these were produced by short-term melting anomalies resulting from temperature fluctuations within the plume [*Jones et al.*, 2014] of 25−30°C over a time scale of circa 8 million years [*Parnell-Turner et al.*, 2014], and not by changes in mantle lithology and fertility [*Foulger et al.*, 2005], or rift propagation and relocation cycles [*Hardarson et al.*, 1997; *Hey et al.*, 2010; *Benediktsdóttir et al.*, 2012].

In the wider North Atlantic, there are three main types of oceanic crust. (1) "Rough" or "normal" oceanic crust with fracture zones separating oceanic ridge segments and a crustal thickness of 6–7 km [*Whitmarsh*, 1971], found to the south of the dashed line in Figure 2a. (2) "Smooth" oceanic crust unbroken by fracture

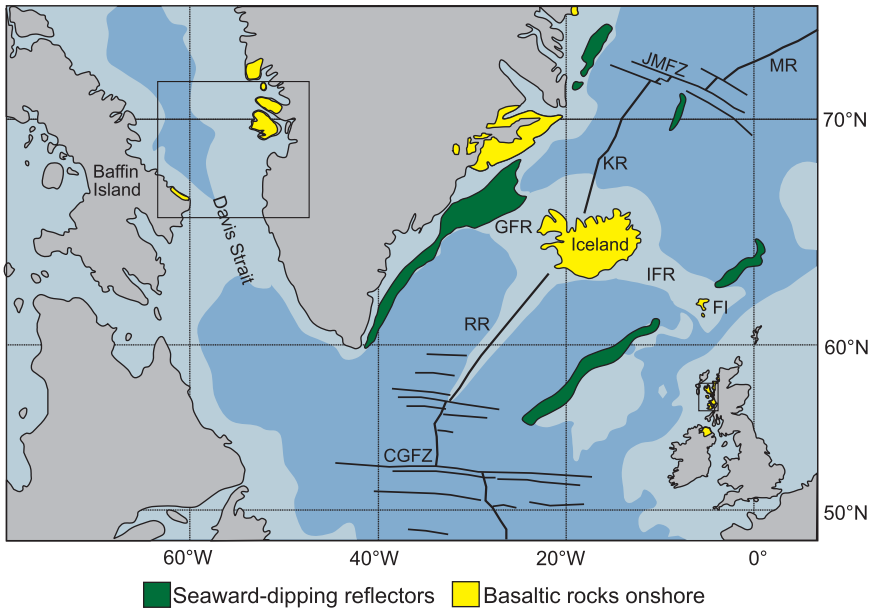

Figure 1. Location of onshore plateau basalts and seaward-dipping reflector sequences in the North Atlantic Igneous Province. The two rectangles show the location of the sample locality maps in Figure 2. CGFZ = Charlie Gibbs Fracture Zone, RR = Reykjanes Ridge, GFR = Greenland-Faeroes Ridge, IFR = Iceland-Faeroes Ridge, FI = Faeroe Islands, KR = Kolbeinsey Ridge, JMFZ = Jan Mayen Fracture Zone, and MR = Mohns Ridge.

zones and found to the north of the dashed line in Figure 2a. This crust is on average 10–11 km thick [*White et al*., 1992] and is thought to have been produced over hotter asthenosphere. (3) Overthickened (20–35 km) oceanic crust that forms the Greenland-Faeroe Ridge (GFR) and the Iceland-Faeroe Ridge (IFR) (Figures 1 and 2a), and is thought to be the result of plume-driven mantle upwelling [*Shorttle and Maclennan*, 2011] and anomalously hot material in the core of the Iceland plume tail [*White and Lovell*, 1997; *Darbyshire et al*., 1998]. The distribution of these three types of crust is variable through time on a longer time scale than the crustal thickness variations recorded by the VSRs. The aim of this study is to use the newly developed Al-in-olivine thermometer to investigate the thermal evolution of the Iceland mantle plume throughout its lifetime and to test whether changes in the large-scale crustal architecture of the North Atlantic region are due to variations in mantle potential temperature (as is the case with the VSRs) as opposed variations in mantle fertility.

2. North Atlantic Bathymetry and Mantle Melting

Oceanic crust up to 30 km thick and represented by seaward-dipping reflectors (Figure 2a) was formed across the entire North Atlantic ocean basin immediately after continental break up at 55 Ma [*Saunders et al*., 1997; *White and Lovell*, 1997], suggesting high mantle temperatures at this time. As the North Atlantic continued to open, seafloor spreading dominated by thinner (6–7 km) fractured oceanic crust, began at 42 Ma [*White and Lovell*, 1997]. To the south of Iceland, this phase was relatively short lived, with a reversion to oceanic crust without fracture zones occurring between 35 and 40 Ma (Figure 2a), suggesting an increase in mantle temperature from this time. The smooth-to-rough transition has continued to extend farther south along the Reykjanes Ridge to the present day, and oceanic crust without fracture zones can now be found >1000 km from Iceland [*White and Lovell*, 1997; *Jones et al*., 2002] suggesting a continuous expansion of the thermal anomaly. Additionally, the width of the broad strip of shallow ocean forming the GFR and IFR has not remained constant through time (Figure 2a). The width of the ridge decreased and was at its narrowest around 35 Ma. There was then a rapid expansion of the ridge into the large oceanic plateau now surrounding Iceland (Figure 2a), suggesting long-term fluctuations in the extent of the thermal anomaly and hence mantle temperature.

Further evidence for long-term temperature changes can be found from a variety of other sources; for example, the rapid decrease in oceanic crustal thickness between 55 and 42 Ma across the region following

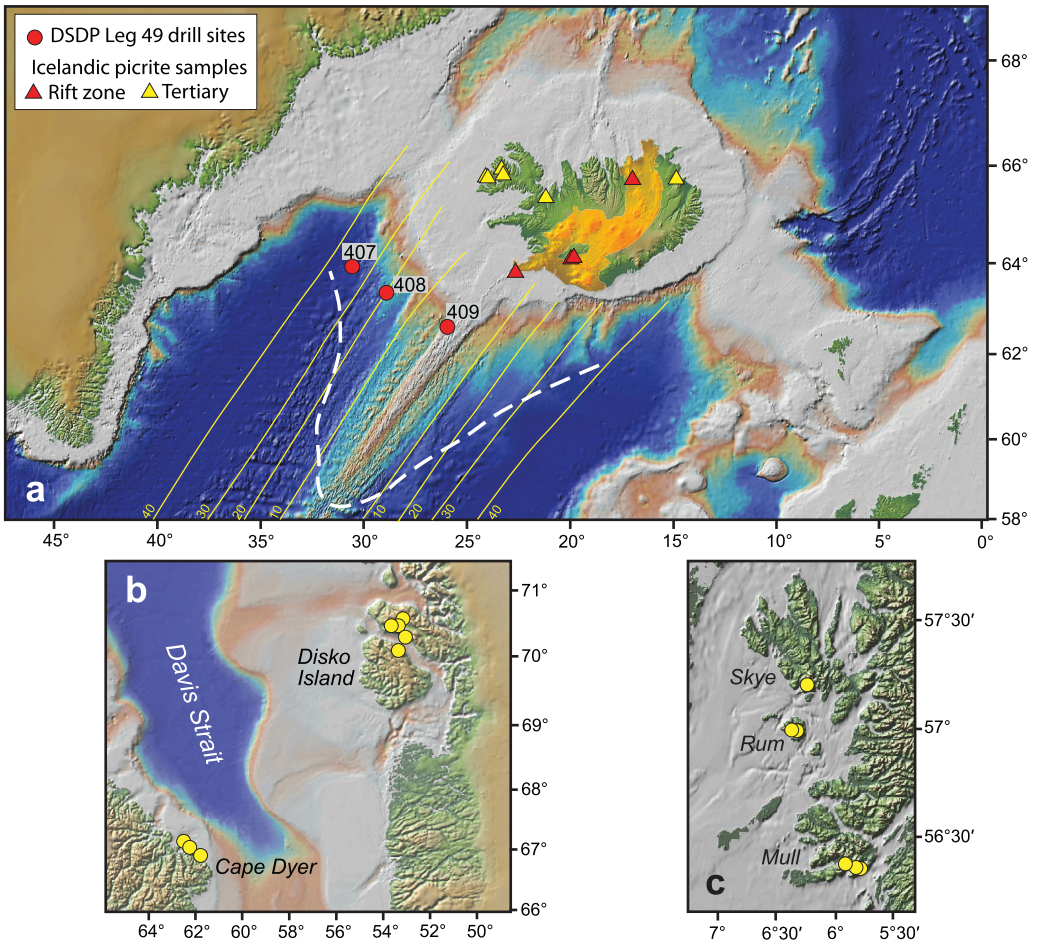

Figure 2. Sample localities and bathymetry of the North Atlantic. (a) Map showing the topography of the seafloor in the North Atlantic region. Iceland sits astride the Mid-Atlantic Ridge and is part of a broad ridge of shallow ocean extending from Greenland to the Faeroe Islands, a result of anomalously hot mantle creating thicker ocean crust. The width of the Greenland-Iceland-Faeroe Ridge decreased until 35 Ma before a rapid expansion to the large oceanic plateau now surrounding Iceland. Yellow lines show the age of the ocean floor (in million years), the white dashed line is the location of the boundary between smooth and rough oceanic crust [*Jones et al*., 2002]. The rough-to-smooth transition has migrated farther southward from Iceland through time, and smooth oceanic crust can now be found more than 1000 km from Iceland. The location of offshore and Iceland sample sites used in this study are indicated. The orange area represents the extent of the neovolcanic zone in Iceland. Maps showing the location of ~61 Ma NAIP picrite samples from (b) West Greenland and Baffin Island and (c) Skye, Mull, and Rum. The location of these areas is shown on Figure 1.

continental break up [*Parkin and White*, 2008]. *Parnell-Turner et al*. [2014] modeled the mantle potential temperature south of Iceland using observed residual water depth anomalies and demonstrated an overall gradual warming since 40 Ma (with superimposed fluctuations related to VSRs), following the sharp decrease in initial temperature of the plume. Additionally, estimates of magmatic flux of the Iceland plume show a rapid decrease from 55 $m^3\ s^{-1}$ immediately post continental break up to 4 $m^3\ s^{-1}$ at 40 Ma, followed by an increase to 7 $m^3\ s^{-1}$ since 23 Ma [*Mjelde and Faleide*, 2009].

3. Estimating Magmatic Temperature

Here we present new thermometry and geochemical data from a suite of rocks spanning the spatial and temporal range of the NAIP to allow us to evaluate temperature fluctuations of the Iceland mantle plume throughout its lifetime. In order to do this, we have selected picrites from three different time periods during the history of the NAIP. These are the most Mg-rich, primitive samples that are known from each location and are most likely to be close in composition to primary melts and therefore to record the highest magmatic temperatures. The suite comprises ~61 Ma picrites from Skye, Rum, Mull, Baffin Island, and West Greenland, which represent the earliest products of NAIP volcanism and arguably the early plume-head

stage of activity (Figures 2b and 2c). The Rum suite includes the M9 dyke studied by *Upton et al*. [2002] which contains the most Mg-rich olivines known from the British Tertiary Igneous Province (BTIP) of up to Fo_{93}. The Baffin Island and West Greenland samples also contain olivine up to Fo_{93}, and have $^3He/^4He$ up to 50 times R_a [*Stuart et al*., 2003; *Starkey et al*., 2009] and are the highest-$^3He/^4He$ volcanic rocks yet found on Earth. The sample suite also includes the ~12–14 Ma high-$^3He/^4He$ Tertiary picrites from Iceland [*Ellam and Stuart*, 2004], and zero-age picrites from the Icelandic neovolcanic zones (Figure 2a). Further information on the samples can be found in the supporting information.

Petrological estimates of magma temperatures have traditionally used olivine-melt Fe-Mg equilibria [*Roeder and Emslie*, 1970; *Ford et al*., 1983; *Beattie*, 1993; *Putirka*, 2005; *Putirka et al*., 2007] and forward and inverse models of peridotite melting [*Herzberg and O'Hara*, 2002; *Green and Falloon*, 2005; *Herzberg et al*., 2007; *Herzberg and Asimow*, 2008, 2015]. While many of these studies have identified thermal anomalies in LIP settings, both approaches require large assumptions regarding melt composition and the pressure at which olivine crystallizes. For example, contrasts in estimates of melt composition have led to very different estimates of mantle temperature at Hawaii [*Falloon et al*., 2007a, 2007b; *Putirka et al*., 2007].

Here we use the Al-in-olivine thermometer calibrated by *Wan et al*. [2008] and extended by *Coogan et al*. [2014]. The Al content of olivine phenocrysts was measured using the Cameca SX100 electron microprobe at the University of Edinburgh. The geothermometer is based solely on the temperature dependence of Al exchange between olivine and Cr-spinel and is largely independent of pressure and melt composition, and so an estimate of these parameters is not required in order to calculate olivine crystallization temperatures. Furthermore, olivine and spinel coprecipitate very early in the crystallization sequence of primitive basalts, likely within a few tens of degrees of the liquidus temperature [*Coogan et al*., 2014]. The thermometer is expressed as:

$$T(^{\circ}\mathrm{C}) = \frac{10000}{0.575 + 0.884 \cdot Cr\# - 0.897 \cdot \ln K_d} - 273, \quad (1)$$

where $Cr = \mathrm{Cr}/(\mathrm{Cr} + \mathrm{Al})$ of spinel in atomic proportions and $K_d = Al_2O_3^{olivine}/Al_2O_3^{spinel}$. The error of the thermometer is estimated to be ±22°C [*Wan et al*., 2008] and includes the error arising from the precision of the olivine Al_2O_3 measurement (0.003–0.0075 wt %).

Example Al-distribution patterns in olivine are shown in Figures 3a and 3b and an example photomicrograph of an olivine from Skye with Cr-spinel inclusions is shown in Figure 3c. The Al_2O_3 content of olivine cores was homogeneous (Figure 3a) in the majority of olivine crystals; however, a small increase in Al was noted up to 100 μm from the contact with the spinel inclusion (Figure 3b), and so analyses were only taken from olivine cores at least 100 μm from Cr-spinel. The cause of this increase close to spinel crystals is unclear, but using the higher Al contents would result in a maximum increase in Al-in-olivine temperature of 30°C and so would not affect the conclusions drawn here.

The Al_2O_3 content and Mg# of primitive (>Fo_{85}) olivines from each sample suite are plotted in Figure 4a. The early NAIP samples (Skye, Mull, Rum, Baffin Island, and West Greenland) have higher olivine Mg# and Al_2O_3 contents than those from Iceland. The 12–14 Ma Iceland olivines plot at systematically lower Al_2O_3 and Mg# than the zero-age olivines. The calculated Al-in-olivine temperature (*T*) plotted against olivine Al_2O_3 content is shown in Figure 4b. It is clear that olivines in the early NAIP crystallized at much higher temperatures than did those from modern Iceland, and that the 12–14 Ma Iceland olivines crystallized at the lowest temperatures. Al-in-olivine *T* is plotted against olivine Mg# in Figure 4c, along with a curve showing how the composition of the olivine responds to falling temperature and fractional crystallization of olivine. This curve was calculated, using PRIMELT3 [*Herzberg and Asimow*, 2015], from the bulk composition of one of the Baffin Island samples (PAD4), which PRIMELT3 shows to be close to its primary magma composition. The magmatic temperature calculated for this sample with PRIMELT3 (1420°C) is the same as we obtain from the same sample using the Al-in-olivine thermometer (Figure 4c). The two olivine phenocrysts in PAD4 that we analyzed are shown circled in Figure 4c. The general positive correlation of the data in Figure 4 and the fit of these data to the fractional crystallization curve could be interpreted as evidence that all the NAIP magmas were produced at the same high temperature and that those samples that record lower temperatures are simply more fractionated. This may explain the few Baffin Island and West Greenland olivines with low Mg# and low temperature, but most of the data from these areas form a horizontal array in Figure 4c and several relatively evolved olivines record some of the highest temperatures. The composition of these olivine cores matches that of the normally zoned olivine rims reported by *Starkey* [2009] in

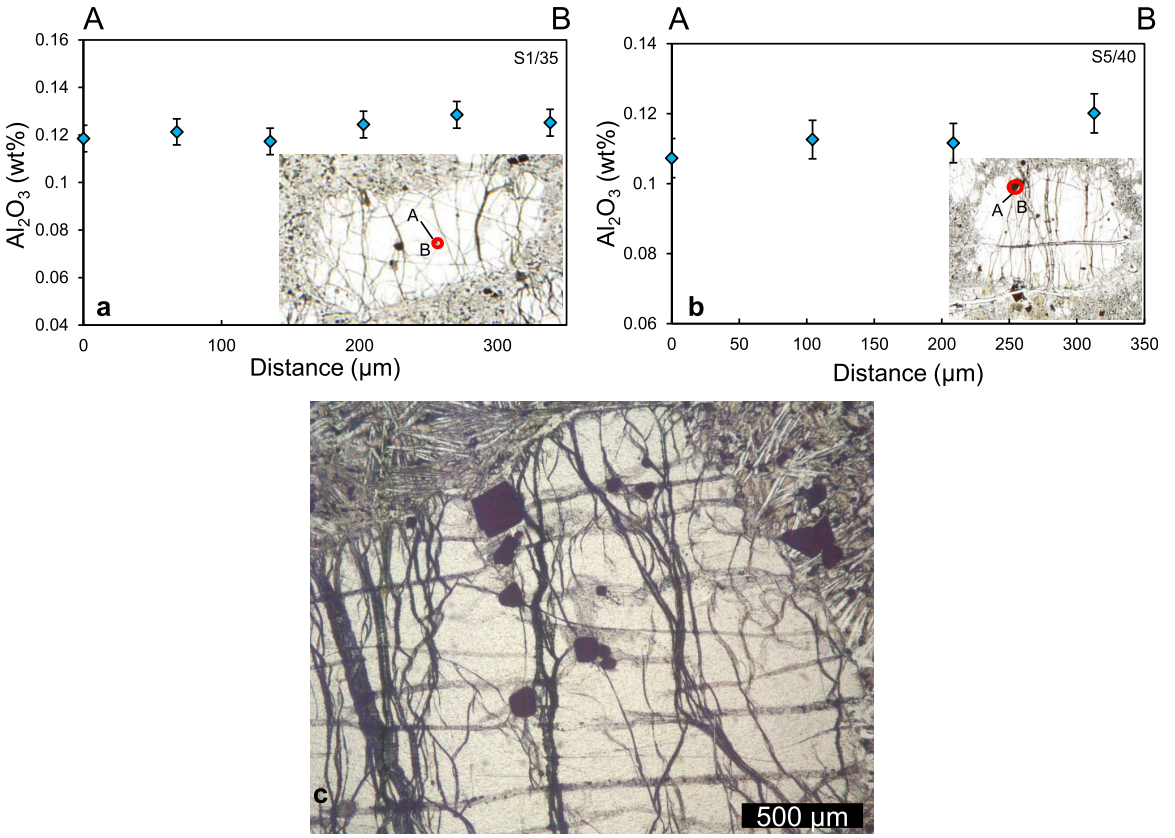

Figure 3. Example photomicrographs and Al-distribution observed in olivine. (a) A typical homogeneous olivine phenocryst from Skye. Most of the olivine crystals are homogeneous in their Al-contents. The transect was taken from A to B. The proximity of the spinel inclusion at B (red circle) has no effect on the Al_2O_3 content of the olivine. (b) An olivine phenocryst with a slight increase in Al-content at the edge of the spinel inclusion. This increase results in an increase in the calculated Al-in-olivine temperature of 30°C. No Fe or Mg zoning is observed. (c) A photomicrograph of a typical olivine phenocryst from Skye. Several Cr-spinel inclusions are easily identifiable by their distinctive red-brown color and cubic crystal form. The olivine crystals are altered to serpentine and iddingsite along fractures but are otherwise unaltered.

the same rocks, and suggests that Fe and Mg in olivine have been reequilibrated by reaction with a more evolved melt. Aluminum, as a trivalent cation, diffuses much more slowly in the olivine lattice [*Spandler and O'Neill*, 2010], and hence the initial high-*T* signature is preserved through the Al content, even when Fe and Mg have reequilibrated. This result demonstrates one of the advantages of using the Al-in-olivine thermometer over olivine-melt Fe-Mg equilibria techniques. We therefore conclude that the temperature variation recorded in the olivines reflects that in the primary magmas and is not due to the effects of fractional crystallization. Further evidence that fractional crystallization was not the dominant process controlling the composition of our picrite samples will be discussed later.

The range in Al_2O_3 content at fixed temperature is a result of variable Cr-spinel compositions. The zero-age Iceland picrites exhibit a bimodal distribution of Al_2O_3 and *T* (Figure 4b) related to geographic location. The higher Al_2O_3 group comprises data from samples erupted in the East Volcanic Zone (EVZ), while data from the lower trend are from picrites from Iceland's North (NVZ) and Reykjanes Volcanic Zones (RVZ). The maximum temperature from each trend is similar; however, the EVZ Cr-spinels tend to have lower Al_2O_3 and higher Cr_2O_3 at fixed *T* when compared to those from the NVZ and RVZ. Cr-spinel compositions in primitive rocks have been shown to be a complex function of magma composition, source composition, fO_2, crystallization temperature, cooling rate and pressure [*Roeder*, 1994], and it is possible that the difference between NVZ and RVZ Cr-spinels and their EVZ counterparts is a reflection of the different melting conditions between these locations. The EVZ is located above the thickest crust [*Darbyshire et al*., 2000], while the RVZ and NVZ picrites were erupted at locations with much lower crustal thicknesses, and hence the melting conditions may have been quite different as crustal thickness influences the depth range of melting.

To illustrate the range of inferred primary magma temperatures across the NAIP, the maximum and average olivine crystallization temperatures calculated using the Al-in-olivine thermometer are compared to MORB

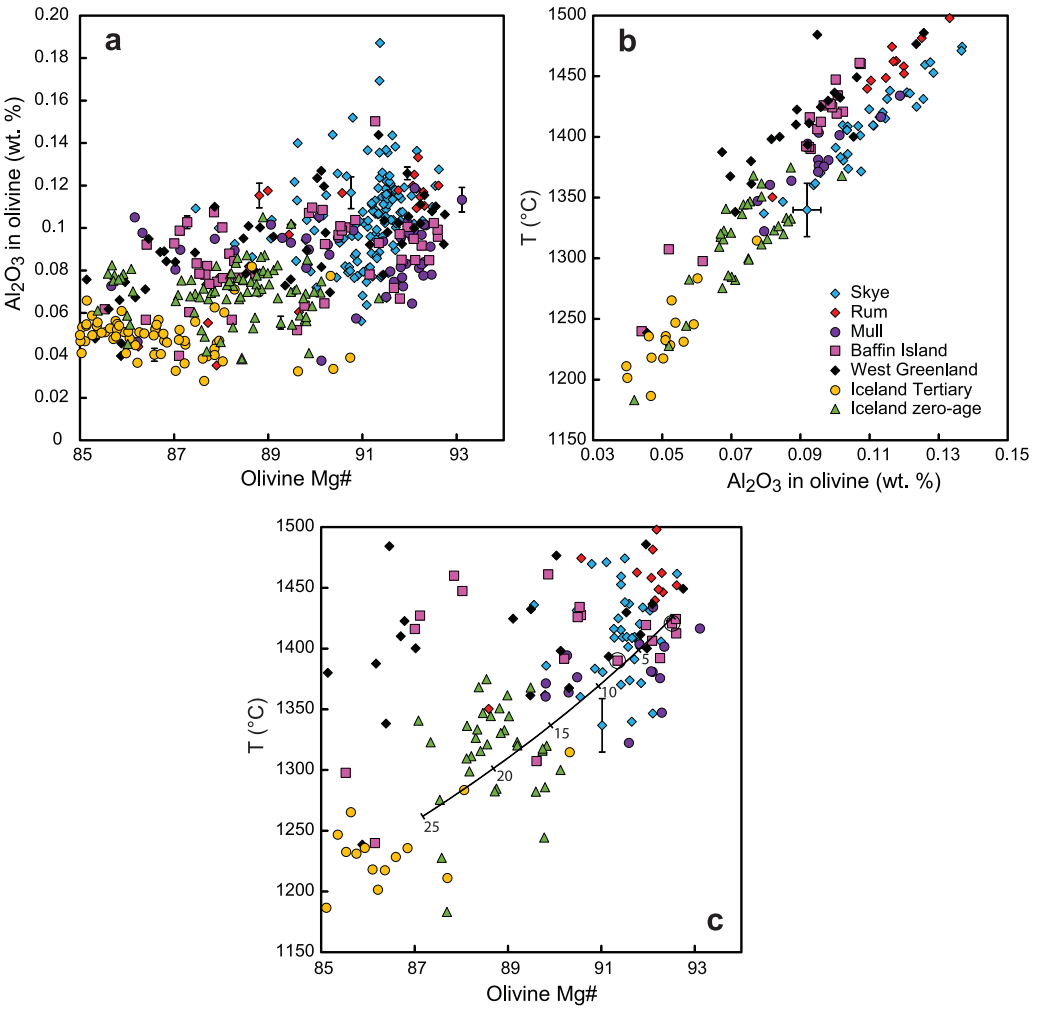

Figure 4. Al-in-olivine results. (a) Al_2O_3 content versus Mg# (Mg# = atomic Mg/(Mg + Fe)) of olivine (>Fo_{85}) from primitive volcanic rocks across the NAIP. Error bars indicate the maximum error in Al_2O_3 content due to the precision of the electron microprobe analyses for representative samples from each suite and are less than the uncertainty in olivine Al_2O_3 measurements of *Wan et al*. [2008]. (b) Al-in-olivine temperature versus olivine Al_2O_3 content. The zero-age Iceland data clearly exhibit an upper and lower trend. (c) Al-in-olivine temperature versus olivine Mg#. The curve shows the effect of falling temperature and fractional crystallization of olivine (numbers are wt % olivine removed) from a primary magma composition calculated from the composition of Baffin Island sample PAD4. The two data points for PAD4 olivines are circled. Primary magma composition and the fractional crystallization curve were calculated using PRIMELT3 [*Herzberg and Asimow*, 2015].

primitive magma values and presented in Table 1 (full results can be found in the supporting information). Our olivine crystallization temperatures for Baffin Island, West Greenland, and present-day Iceland are similar to primary magma temperatures obtained by *Herzberg and O'Hara* [2002] and *Herzberg et al*. [2007] by their forward and inverse modeling technique. In the next section, we argue that our results reflect variation in mantle potential temperature (*Tp*), the temperature of the mantle if it were able to reach the Earth's surface decompressed and unmelted [*McKenzie and Bickle*, 1988].

4. Relationship of Magmatic Temperature to Mantle Potential Temperature

Converting olivine crystallization temperature to *Tp* requires assumptions about the depth at which the olivine phenocrysts crystallized and the depth and degree of melting, all of which are difficult to constrain accurately. Olivine crystallization temperature increases with pressure at a rate of about 50 °C/GPa or about 1.7 °C/km [*Herzberg and O'Hara*, 2002; *Asimow and Longhi*, 2004], so most of the range of temperature that we measured could theoretically be due to systematic variation in the depth at which olivine in the various parts of the NAIP crystallized. However, this would require that most of the olivine phenocrysts in the older

Table 1. Temperatures Calculated Using the Al-in-Olivine Thermometer for Each Suite of Picrite[a] and Comparison With MORB Primitive Magma T[b]

Sample Suite	T_{max}	ΔT^{c}_{max}	$\Delta T^{d}_{average}$
Skye	1474	278	217
Mull	1434	241	187
Rum (M9)	1498	305	259
Baffin Island	1461	268	207
West Greenland	1486	291	213
Iceland 13-14 Ma	1314	122	44
Iceland zero-age	1368	175	122

[a]The likely error in our temperature estimates is ±22°C.
[b]The average Al-in-olivine T of MORB primitive magma is calculated to be 1193°C [*Coogan et al.*, 2014].
[c]ΔT_{max} = max Al-in-olivine T for each suite—T_{MORB}.
[d]$\Delta T_{average}$ = average Al-in-olivine T of each suite—T_{MORB}.

parts of the NAIP crystallized at considerable depth whereas those in Iceland crystallized at much shallower levels. Many of the olivine crystals in the Baffin Island and West Greenland picrites have elongate and skeletal morphology indicating rapid growth, probably just before or during eruption. Furthermore, the 1.7 °C/km increase in the temperature of olivine crystallization is greater than the adiabatic gradient of about 1 °C/km in basaltic magmas and so the primitive magmas are likely to remain at or above their liquidus temperature during ascent. Therefore, any olivine phenocrysts that crystallize at depth from high-temperature magmas are unlikely to survive ascent to the surface, and certainly will not dominate the observed phenocryst population.

It is possible that some of the observed variation in magma temperature is due to variations in lithosphere thickness, and hence the depth at which the magmas formed, rather than variation in mantle potential temperature. The smallest melt fractions will be produced as the upwelling mantle crosses its solidus and so olivine crystallizing from these melts will record the highest temperatures. As decompression progresses, increasing melt fraction will be accompanied by a fall in magma temperature as heat is used to convert solid to liquid. Thus, the largest melt fractions will have the lowest temperatures. The drop in temperature resulting from 25% melting will be around 140 °C [*McKenzie and Bickle*, 1988]. If this effect is dominant in our data, we should expect a *positive* correlation between temperature and the concentration of incompatible elements because the latter would be highest in the smallest melt fractions and lowest in the largest fractions. The same positive correlation should thus be seen in the case where variation in measured magmatic temperature is the result of variable lithosphere thickness but constant *Tp*. Conversely, if *Tp* varies but lithosphere thickness remains constant, we should expect to see a *negative* correlation between magmatic temperature and the concentration of incompatible elements because the largest melt fractions will result from the highest *Tp*.

In Figures 5a and 5b, we plot bulk-rock Zr concentration and Zr/Y, respectively, against the individual temperature estimates for each picrite sample. We chose Zr because it is moderately incompatible and therefore sensitive to the large melt fraction variations expected during decompression melting in plumes, but not very sensitive to variations in relative enrichment or depletion in the mantle sources, which affect highly incompatible elements to a much greater extent. Zr/Y is likewise sensitive to degree of melting but is insensitive to the effects of the fractional crystallization or accumulation of olivine because both Zr and Y are highly incompatible in olivine ($D \approx 0$). Figures 5c and 5d show that Zr and Zr/Y both correlate inversely with Mg# as would be expected from variation in melt fraction. The effects of olivine fractional crystallization are shown in Figure 5c as a curve that was calculated by subtracting 0.1 wt % increments of equilibrium olivine from one of the Baffin Island samples (PAD4) [*Starkey et al.*, 2009]. The curve lies obliquely to the data array, showing that olivine fractional crystallization was not dominant in determining the composition of our picrite samples. Similarly, the inverse correlation between Zr/Y and bulk-rock Mg# (Figure 5d) shows that olivine accumulation cannot have been a dominant process either.

The lack of any correlation between our temperature estimates and Zr concentration or Zr/Y (Figures 5a and 5b) suggests that the observed temperature variation is not dominated by the cooling effect of decompression melting but must reflect variations in both *Tp* and lithosphere thickness. The spread of data most likely results from the combined effects of *Tp* variation, variable lithosphere thickness, and the mixing of individual melt increments, each containing olivine phenocrysts. Since the total temperature reduction in individual melt increments generated during decompression melting is likely to be <140 °C [*McKenzie and Bickle*, 1988], the variation in the temperature of aggregate melts due to variation in lithosphere thickness will be much less than this, and therefore much less than the range of temperatures reported here. We conclude that the temperature variations that we see are dominated by variation in mantle *Tp* and therefore our maximum Al-in-olivine temperatures can be used as a proxy for mantle *Tp*. Our data suggest a

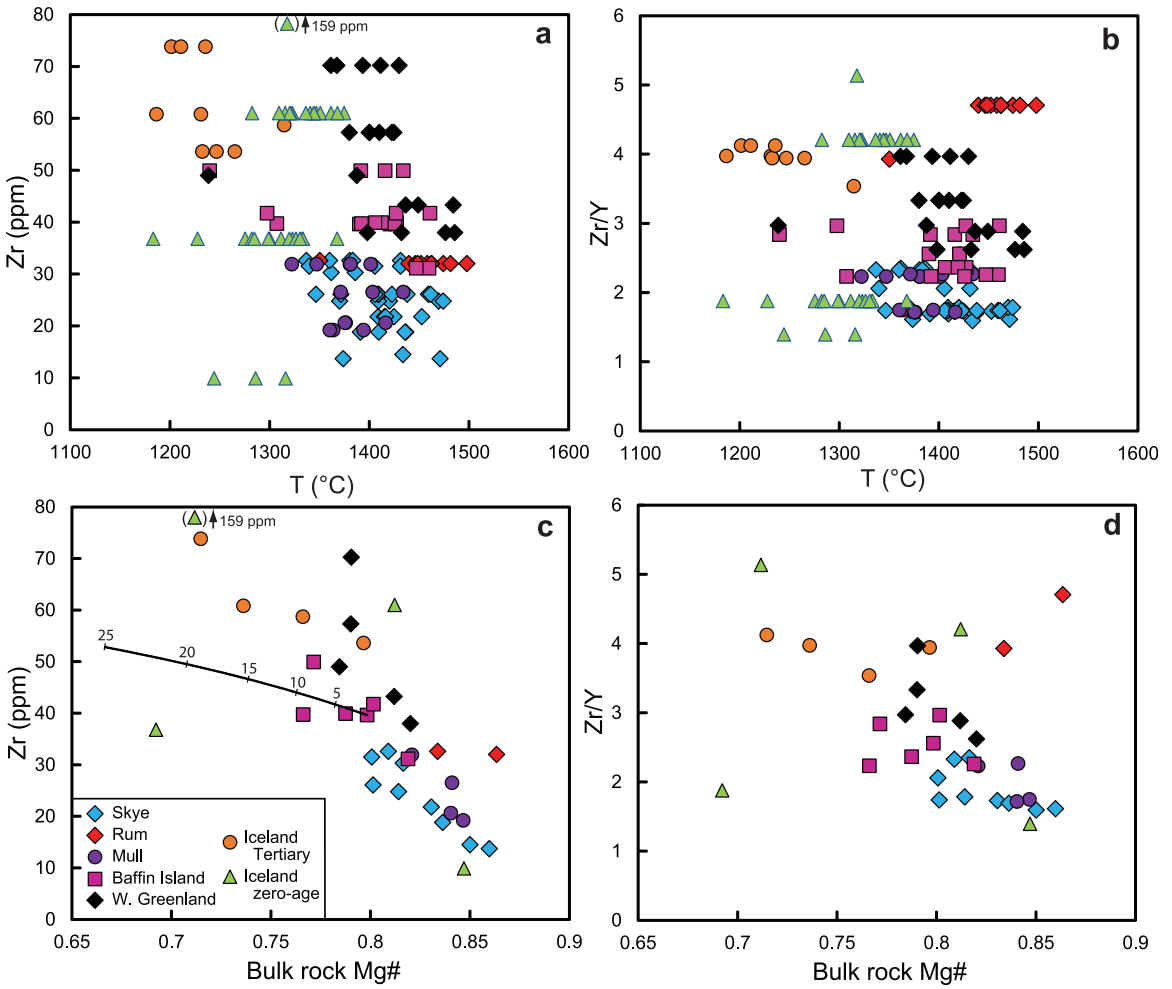

Figure 5. Variation of (a) Zr concentration and (b) Zr/Y with temperature for picrites from the NAIP. Zr and Zr/Y measured in the host rocks are plotted against individual temperature estimates based on the Al-in-olivine geothermometer. A positive correlation would be expected if the measured temperature variation were due solely to variation in depth of olivine crystallization (a function of lithosphere thickness) rather than variation in mantle potential temperature. (c) Zr concentration and (d) Zr/Y are inversely correlated with Mg# in the host rocks as would be expected with large variations in melt fraction. The curve in Figure 5c shows the effect of fractional crystallization of olivine ($D_{Zr} = 0$; numbers are wt % olivine extracted) from a magma represented by one of the Baffin Island samples (PAD4). Figures 5c and 5d show that neither fractional crystallization nor accumulation of olivine can be the dominant factor controlling the composition of the magmas because the curve in Figure 5c is oblique to the data array, and Zr/Y is insensitive to both processes because both Zr and Y are highly incompatible in olivine. Mg# is mol MgO/(mol MgO + mol FeO); FeO is calculated by assuming that FeO = 0.9FeO* where FeO* is total Fe calculated as FeO.

widespread thermal anomaly with Al-in-olivine *T* up to ~300 °C above that of average MORB primitive magma, and therefore a *Tp* anomaly of similar magnitude, across the NAIP at the onset of volcanism at 61 Ma. Our estimated maximum temperature anomaly in present-day Icelandic picritic magmas (175 °C; Table 1) is close to the excess mantle temperature (186 °C) beneath Iceland estimated by *Putirka et al.* [2007] using olivine-liquid equilibria.

The temperature estimates for the BTIP are as high as those calculated for Baffin Island and West Greenland, despite their being separated by a distance of ~2000 km at 61 Ma. West Greenland is estimated to have been close to the plume center at 61 Ma [*Lawver and Müller*, 1994], whereas the BTIP was the farthest away from it. This observation suggests that the high-temperature plume head spread rapidly over a wide area at 61 Ma and that the temperature distribution within the plume head was uniform. Our data support numerical modeling by *Larsen et al.* [1999] who argued that the simultaneous onset of volcanism across the NAIP at 61–62 Ma could be explained by a fast moving plume head that spread out horizontally at a rate of 0.5 m/yr upon impact with the lithosphere. The data also support models that predict that rising mantle plume heads are ~300 °C hotter than surrounding ambient mantle, and quickly flatten to form disks with diameters of 2000–2500 km upon arrival at the base of the lithosphere [*White and McKenzie*, 1989; *Campbell*, 2007]. However, we do not see a decrease in temperature from the center of the plume as predicted by

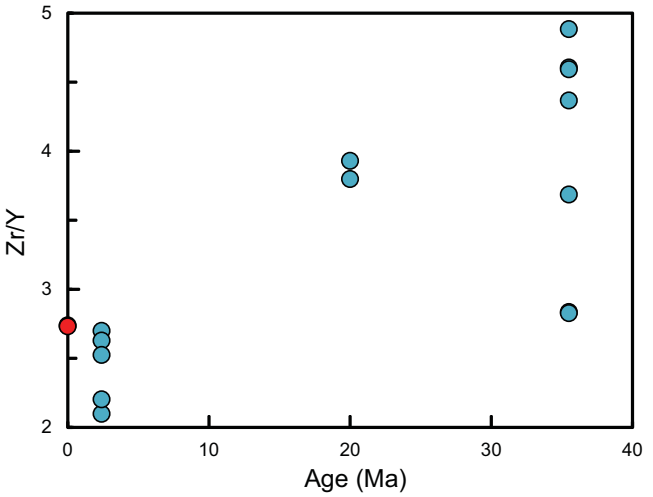

Figure 6. Zr/Y versus age for basalt samples collected along a mantle flow line extending west from the Reykjanes Ridge. Data from samples recovered during DSDP Leg 49 (Sites 407, 408, and 409) are shown with blue circles; the red circle represents basalt dredged from the ridge axis along the same flow line (close to Site 409). The location of the DSPD sites is shown on Figure 2a.

Campbell [2007], but we cannot rule out the possibility that lower temperature mantle even more distal than the BTIP simply did not melt.

The Al-in-olivine thermometry data indicate that the mantle plume significantly cooled down after the initial plume-head phase of activity at ~61 Ma in agreement with the narrowing of the GFR and IFR until 35 Ma (Figure 2a). Picritic basalts from the far northwest and northeast of Iceland represent some of the oldest rocks on the island (12–14 Ma) and record the lowest temperatures of all the samples in this study. Recent picrites and primitive basalts from Iceland's active neovolcanic zones record a 54 °C increase in maximum olivine-Cr-spinel cosaturation temperature, and an average increase of 78 °C since the 12–14 Ma samples were erupted. This conclusion is in agreement with the southward migration of the smooth-to-rough oceanic crust boundary since 40–35 Ma.

5. Temporal Variation in the Composition of Reykjanes Ridge Basalts

Geochemical data for basalt samples recovered from the North Atlantic south of Iceland provide further support for an increase in mantle temperature since 35 Ma. Three sites (407, 408, and 409) were drilled on the western flank of the Reykjanes Ridge along a mantle flow line away from the ridge crest during Deep Sea Drilling Program (DSDP) Leg 49 [*Luyendyk et al*., 1978] shown on Figure 2a. Figure 6 shows the variation with age of Zr/Y [*Kempton et al*., 2000], which decreases with increasing melt fraction and hence mantle temperature, for these samples together with the composition of zero-age basalt [*Murton et al*., 2002] dredged from the Reykjanes Ridge axis at 62.6 °N (close to DSDP Site 409; Figure 2a) on the same mantle flow line. Zr/Y varies during the melting of spinel lherzolite but is insensitive to low-pressure fractional crystallization of olivine and plagioclase, in which both Zr and Y are highly incompatible. Zr/Y measured in the basalt samples will therefore be the same as in the primary magmas. The decrease in Zr/Y with time is consistent with an increase in mantle temperature over the past 35 Ma.

Using the Zr/Y data in Figure 6 to estimate the variation in mantle temperature is far from straightforward because we do not know the mantle composition or what portions of the whole melt column are represented by the basalts. However, we can make some simple assumptions to derive a rough estimate of the magnitude of temperature variation. We assume a mantle source with 9 ppm Zr and 4 ppm Y; slightly more enriched than the depleted mantle composition estimated by *Salters and Stracke* [2004] and similar to the mantle source for primitive Ontong Java Plateau basalt [*Fitton and Godard*, 2004]. Because most of the melting beneath spreading centers takes place in the spinel lherzolite stability field, we have estimated bulk distribution coefficients on the assumption that Zr and Y are contained mostly in clinopyroxene. Our values for Zr (0.019) and Y (0.06) were based on averages of recently published data. A simple batch melting equation, spinel lherzolite mineral proportions given by *McKenzie and O'Nions* [1991] and spinel lherzolite melting modes from *Baker and Stolper* [1994] was used. With these assumptions we find that the observed variation in Zr/Y from ~4 between 35 and 20 Ma to ~2.5 at present equates to an increase in melt fraction from 0.03 to 0.15. The lower value (0.03) is too low for the formation of ocean crust, implying the involvement of garnet (with a much higher D-value for Y) in the deeper parts of the melt column, but the upper value is more robust. The range in F (0.03–0.15) would

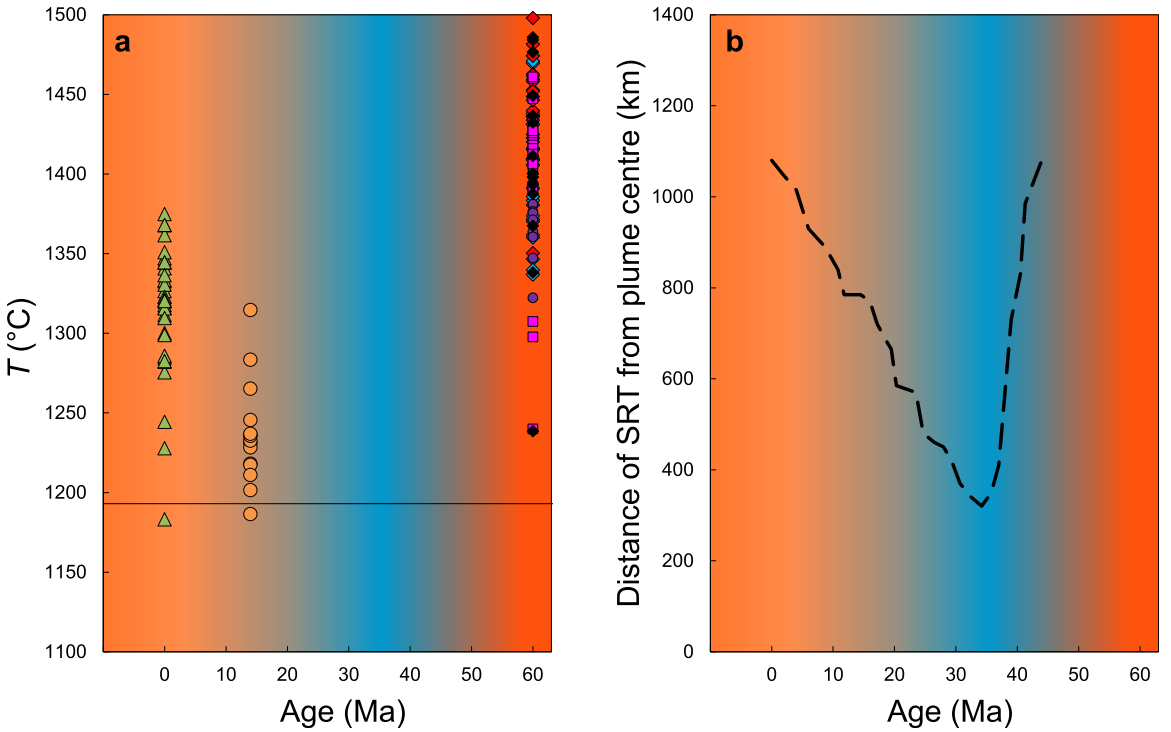

Figure 7. Summary of age and temperature data. (a) Age versus Al-in-olivine temperature. Symbols as in Figure 4. Average MORB primitive magma *T* is indicated by the horizontal line. The background colors provide a schematic indication of North Atlantic mantle temperatures, with orange indicating highest temperatures and blue indicating the lowest temperatures. (b) Age versus distance from the plume center under Iceland to the smooth-to-rough transition (SRT) in the ocean crust [*Jones et al.*, 2002]. The boundary is at a minimum distance from Iceland at ~35 Ma, our best estimate for the age at which the mantle plume was at its coolest. Since ~35 Ma, the boundary has migrated gradually southward, away from Iceland, indicating increasing mantle temperatures and an expansion in the area influenced by the thermal anomaly associated with the plume.

require an increase in mantle potential temperature of around 100 °C at 1 GPa based on parameterization of anhydrous melting experiments by *Katz et al.* [2003, Figure 11]. Given that this is a maximum temperature increase due to the likely involvement of garnet, it is comparable with the temperature increase (54−78 °C) that we estimate from the Al-in-olivine thermometer in Icelandic picrite between 14 Ma and the present.

6. Temperature of the Iceland Mantle Plume Through Time

Compiling all the available data, we present a temperature versus age diagram for the NAIP (Figure 7a). We estimate that minimum mantle temperatures were experienced at around 40–35 Ma based on the range of evidence presented here, including the migration southward of the smooth-to-rough oceanic crustal boundary since 35 Ma (Figure 7b). It has previously been recognized that the VSRs south of Iceland represent short-term temperature fluctuations in the Iceland plume. We have shown that large-scale changes in the crustal architecture of the North Atlantic region can be explained by long-term cooling of the Iceland plume to 35 Ma, followed by a gradual increase in temperatures until the present day. This suggests that mantle plumes are susceptible to long-term (10^7 year) fluctuations in temperature throughout their lifetime.

At the onset of volcanism in the NAIP, caused by the arrival of the plume head at the base of the lithosphere, a large thermal anomaly several hundred degrees above that of ambient mantle extended across a 2000 km wide area. The Al-in-olivine thermometry data thus confirm that start-up plumes are associated with a pulse of anomalously hot mantle over a large spatial area before becoming focused into a narrow upwelling. These conclusions are independent of traditional petrologic approaches to mantle temperature estimation, and provide another strong piece to the growing body of evidence indicating that the temperature of the mantle source region of LIPs is substantially higher than that beneath the mid-ocean ridges.

Acknowledgments
We thank Lotte Larsen, Brian Upton, Fin Stuart, Thor Thordarson, and Björn Hardarson for providing samples, Christopher Hayward for his assistance with electron microprobe analyses, Nic Odling for carrying out XRF analysis, Mike Hall for preparing polished thin sections, and Jen Brooke and Tom Barraclough for their assistance with fieldwork. We are also grateful to John Maclennan, Oliver Shorttle, Keith Putirka, and an anonymous reviewer for their constructive and very helpful reviews of the manuscript, and to Janne Bilchert-Toft for editorial handling. The data used in this paper can be found in the supporting information. The work was supported by a PhD studentship from the UK Engineering and Physical Sciences Research Council.

References

Asimow, P. D., and J. Longhi (2004), The significance of multiple saturation points in the context of polybaric near-fractional melting, *J. Pet.*, *45*, 2349–2367, doi:10.1093/petrology/egh043.

Baker, M. B., and E. M. Stolper (1994), Determining the composition of high-pressure mantle melts using diamond aggregates, *Geochim. Cosmochim. Acta*, *58*, 2811–2827, doi:10.1016/0016-7037(94)90116-3.

Beattie, P. (1993), Olivine-melt and orthopyroxene-melt equilibria, *Contrib. Mineral. Petrol.*, *115*, 103–111, doi:10.1007/BF00712982.

Benediktsdóttir, A., R. Hey, F. Martinez, and A. Höskuldsson (2012), Detailed tectonic evolution of the Reykjanes Ridge during the past 15 Ma, *Geochem. Geophys. Geosyst.*, *13*, Q02008, doi:10.1029/2011GC003948.

Campbell, I. H. (2007), Testing the plume theory, *Chem. Geol.*, *241*, 153–176, doi:10.1016/j.chemgeo.2007.01.024.

Coogan, L. A., A. D. Saunders, and R. N. Wilson (2014), Aluminium-in-olivine thermometry of primitive basalts: Evidence of an anomalously hot mantle source for large igneous provinces, *Chem. Geol.*, *368*, 1–10, doi:10.1016/j.chemgeo.2014.01.004.

Darbyshire, F. A., I. Bjarnason, R. S. White, and Ó. G. Flóvenz, (1998), Crustal structure above the iceland mantle plume imaged by the ICE-MELT refraction profile, *Geophys. J. Int.*, *135*, 1131–1149, doi:10.1046/j.1365-246X.1998.00701.x.

Darbyshire, F. A., R. S. White, and K. F. Priestley (2000), Structure of the crust and uppermost mantle of Iceland from a combined seismic and gravity study, *Earth Planet. Sci. Lett.*, *181*, 409–428, doi:10.1016/S0012-821X(00)00206-5.

Ellam, R. M., and F. M. Stuart (2004), Coherent He-Nd-Sr isotope trends in high $^{3}He/^{4}He$ basalts: Implications for a common reservoir, mantle heterogeneity and convection, *Earth Planet. Sci. Lett.*, *228*, 511–523, doi:10.1016/j.epsl.2004.10.020.

Falloon, T. J., L. V. Danyushevsky, A. Ariskin, D. H. Green, and C. E. Ford (2007a), The application of olivine geothermometry to infer crystallization temperatures of parental liquids: Implications for the temperature of MORB magmas, *Chem. Geol.*, *241*, 207–233, doi:10.1016/j.chemgeo.2007.01.015.

Falloon, T. J., D. H. Green, and L. V. Danyushevsky (2007b), Crystallization temperatures of tholeiite parental liquids: Implications for the existence of thermally driven mantle plumes, *Geol. Soc. Am. Spec. Pap.*, *430*, 235–260, doi:10.1130/2007.2430(12).

Fitton, J. G., and M. Godard (2004), Origin and evolution of magmas on the Ontong Java Plateau, in *Origin and Evolution of the Ontong Java Plateau*, edited by J. G. Fitton et al., *Geol. Soc. Spec. Publ., 229*, 151–178, doi:10.1144/GSL.SP.2004.229.01.10.

Ford, C. E., D. G. Russell, J. A. Craven, and M. R. Fisk (1983), Olivine-liquid equilibria: Temperature, pressure and composition dependence of the crystal/liquid cation partition coefficients for Mg, Fe^{2+}, Ca and Mn, *J. Pet.*, *24*, 256–266, doi:10.1093/petrology/24.3.256.

Foulger, G. R., and D. L. Anderson (2005), A cool model for the Iceland hotspot, *J. Volcanol. Geotherm. Res.*, *141*, 1–22, doi:10.1016/j.jvolgeores.2004.10.007.

Foulger, G. R., J. H. Natland, and D. L. Anderson (2005), A source for Icelandic magmas in remelted Iapetus crust, *J. Volcanol. Geotherm. Res.*, *141*, 23–44, doi:10.1016/j.jvolgeores.2004.10.006.

Green, D. H., and T. J. Falloon (2005), Primary magmas at mid-ocean ridges, "hotspots", and other intraplate settings: Constraints on mantle potential temperature, *Geol. Soc. Am. Spec. Pap.*, *288*, 217–247, doi:10.1130/0-8137-2388-4.217.

Hardarson, B. S., J. G. Fitton, R. M. Ellam, and M. S. Pringle (1997), Rift relocation—A geochemical and geochronological investigation of a palaeo-rift in northwest Iceland, *Earth Planet. Sci. Lett.*, *153*, 181–196, doi:10.1016/S0012-821X(97)00145-3.

Herzberg, C., and P. D. Asimow (2008), Petrology of some oceanic island basalts: PRIMELT2.XLS software for primary magma calculation, *Geochem. Geophys. Geosyst.*, *9*, Q09001, doi:10.1029/2008GC002057.

Herzberg, C., and P. D. Asimow (2015), PRIMELT3 MEGA.XLSM software for primary magma calculation: Peridotite primary magma MgO contents from the liquidus to the solidus, *Geochem. Geophys. Geosyst.*, *16*, 563–578, doi:10.1002/2014G005631.

Herzberg, C., and M. J. O'Hara (2002), Plume-associated ultramafic magmas of Phanerozoic age, *J. Pet.*, *43*, 1857–1883, doi:10.1093/petrology/43.10.1857.

Herzberg, C., P. D. Asimow, N. Arndt, Y. Niu, C. M. Lesher, J. G. Fitton, M. J. Cheadle, and A. D. Saunders (2007), Temperatures in ambient mantle and plumes: Constraints from basalts, picrites, and komatiites, *Geochem. Geophys. Geosyst.*, *8*, Q02006, doi:10.1029/2006GC001390.

Hey, R., F. Martinez, A. Höskuldsson, and A. Benediktsdóttir (2010), Propagating rift model for the V-shaped ridges south of Iceland, *Geochem. Geophys. Geosyst.*, *11*, Q03011, doi:10.1029/2009GC002865.

Jones, S. M., N. White, and J. Maclennan (2002), V-shaped ridges around Iceland: Implications for spatial and temporal patterns of mantle convection, *Geochem. Geophys. Geosyst.*, *3*(10), 1059, doi:10.1029/2002GC000361.

Jones, S. M., B. J. Murton, J. G. Fitton, N. J. White, J. Maclennan, and R. L. Walters (2014), A joint geochemical-geophysical record of time-dependent mantle convection south of Iceland, *Earth Planet. Sci. Lett.*, *386*, 86–97, doi:10.1016/j.epsl.2013.09.029.

Katz, R. F., M. Spiegelman, and C. H. Langmuir (2003), A new parameterization of hydrous mantle melting, *Geochem. Geophys. Geosyst.*, *4*(9), 1073, doi:10.1029/2002GC000433.

Kempton, P. D., J. G. Fitton, A. D. Saunders, G. M. Nowell, R. N. Taylor, B. S. Hardarson, and G. Pearson (2000), The Iceland plume in space and time: A Sr-Nd-Hf-Pb study of the North Atlantic rifted margin, *Earth Planet. Sci. Lett.*, *177*, 255–271, doi:10.1016/S0012-821X(00)00047-9.

Larsen, T. B., D. A. Yuen, and M. Storey (1999), Ultrafast mantle plumes and implications for flood basalt volcanism in the Northern Atlantic Region, *Tectonophysics*, *311*, 31–43, doi:10.1016/S0040-1951(99)00163-8.

Lawver, L. A., and R. D. Müller (1994), Iceland hotspot track, *Geology*, *22*, 311–314, doi:10.1130/0091-7613(1994)022 < 0311:IHT>2.3.CO;2.

Luyendyk, B. P., et al. (1978), *Initial Reports of the Deep Sea Drilling Project*, vol. 49, U.S. Gov. Print. Off., Washington, D. C.

McKenzie, D., and M. J. Bickle (1988), The volume and composition of melt generated by extension of the lithosphere, *J. Pet.*, *29*, 625–679, doi:10.1093/petrology/29.3.625.

McKenzie, D., and R. K. O'Nions (1991), Partial melt distributions from inversion of rare earth element concentrations, *J. Pet.*, *32*, 1021–1091, doi:10.1093/petrology/32.5.1021.

Mjelde, R., and J. I. Faleide (2009), Variation of Icelandic and Hawaiian magmatism: Evidence for co-pulsation of mantle plumes?, *Mar. Geophys. Res.*, *30*, 61–72, doi:10.1007/s11001-009-9066-0.

Murton, B. J., R. N. Taylor, and M. F. Thirwall (2002), Plume-ridge interaction: A geochemical perspective from the Reykjanes Ridge, *J. Pet.*, *43*, 1987–2012, doi:10.1093/petrology/43.11.1987.

Parkin, C. J., and R. S. White (2008), Influence of the Iceland mantle plume on oceanic crust generation in the North Atlantic, *Geophys. J. Int.*, *173*, 168–188, doi:10.1111/j.1365-246X.2007.03689.x.

Parnell-Turner, R., N. White, T. Henstock, B. Murton, J. Maclennan, and S. M. Jones (2014), A continuous 55-million-year record of transient mantle plume activity beneath Iceland, *Nat. Geosci.*, *7*, 914–919, doi:10.1038/ngeo2281.

Putirka, K. D. (2005), Mantle potential temperatures at Hawaii, Iceland, and the mid-ocean ridge system, as inferred from olivine phenocrysts: Evidence for thermally driven mantle plumes, *Geochem. Geophys. Geosyst.*, *6*, Q05L08, doi:10.1029/2005GC000915.

Putirka, K. D., M. Perfit, F. J. Ryerson, and M. G. Jackson (2007), Ambient and excess mantle temperatures, olivine thermometry, and active vs. passive upwelling, *Chem. Geol.*, *241*, 177–206, doi:10.1016/j.chemgeo.2007.01.014.

Roeder, P. L. (1994), Chromite; from the fiery rain of chondrules to the Kilauea Iki lava lake, *Can. Mineral.*, *32*, 729–746.

Roeder, P. L., and R. F. Emslie (1970), Olivine-liquid equilibrium, *Contrib. Mineral. Petrol.*, *29*, 275–289, doi:10.1007/BF00371276.

Salters, V. J. M., and A. Stracke (2004), Composition of the depleted mantle, *Geochem. Geophys. Geosyst.*, *5*, Q05B07, doi:10.1029/2003GC000597.

Saunders, A., J. Fitton, A. Kerr, M. Norry, and R. Kent (1997), The North Atlantic Igneous Province, in *Large Igneous Provinces: Continental, Oceanic, and Planetary Flood Volcanism*, edited by J. J. Mahoney and M. F. Coffin, pp. 45–93, AGU, Washington, D. C., doi:10.1029/GM100p0045.

Shorttle, O., and J. Maclennan (2011), Compositional trends of Icelandic basalts: Implications for short-length scale lithological heterogeneity in mantle plumes, *Geochem. Geophys. Geosyst.*, *12*, Q11008, doi:10.1029/2011GC003748.

Spandler, C., and H. S. C. O'Neill (2010), Diffusion and partition coefficients of minor and trace elements in San Carlos olivine at 1300 °C with some geochemical implications, *Contrib. Mineral. Petrol.*, *159*, 791–818, doi:10.1007/s00410-009-0456-8.

Starkey, N. (2009), Evolution of the Earth's mantle-crust-atmosphere system from the trace element and isotope geochemistry of the plume-mantle reservoir, PhD thesis, Univ. of Edinburgh, Edinburgh.

Starkey, N. A., F. M. Stuart, R. M. Ellam, J. G. Fitton, S. Basu, and L. M. Larsen (2009), Helium isotopes in early Iceland plume picrites: Constraints on the composition of high $^{3}He/^{4}He$ mantle, *Earth Planet. Sci. Lett.*, *277*, 91–100, doi:10.1016/j.epsl.2008.10.007.

Stuart, F. M., S. Lass-Evans, J. G. Fitton, and R. M. Ellam (2003), High $^{3}He/^{4}He$ ratios in picritic basalts from Baffin Island and the role of a mixed reservoir in mantle plumes, *Nature*, *424*, 57–59, doi:10.1038/nature01711.

Upton, B. G. J., A. C. Skovgaard, J. McClurg, L. Kirstein, M. Cheadle, C. H. Emeleus, W. J. Wadsworth, and A. E. Fallick (2002), Picritic magmas and the Rum ultramafic complex, Scotland, *Geol. Mag.*, *139*, 437–452, doi:10.1017/S0016756802006684.

Vogt, P. R. (1971), Asthenosphere motion recorded by the ocean floor south of Iceland, *Earth Planet. Sci. Lett.*, *13*, 153–160, doi:10.1016/0012-821X(71)90118-X.

Wan, Z., L. A. Coogan, and D. Canil (2008), Experimental calibration of aluminium partitioning between olivine and spinel as a geothermometer, *Am. Mineral.*, *93*, 1142–1147, doi:10.2138/am.2008.2758.

White, N., and B. Lovell (1997), Measuring the pulse of a plume with the sedimentary record, *Nature*, *387*, 888–891.

White, R., and D. McKenzie (1989), Magmatism at rift zones: The generation of volcanic continental margins and flood basalts, *J. Geophys. Res.*, *94*, 7685–7729, doi:10.1029/JB094iB06p07685.

White, R. S., D. McKenzie, and R. K. O'Nions (1992), Oceanic crustal thickness from seismic measurements and rare earth element inversions, *J. Geophys. Res.*, *97*, 19,683–19,715, doi:10.1029/92JB01749.

White, R. S., J. W. Brown, and J. R. Smallwood (1995), The temperature of the Iceland plume and origin of outward-propagating V-shaped ridges, *J. Geol. Soc.*, *152*, 1039–1045, doi:10.1144/GSL.JGS.1995.152.01.26.

Whitmarsh, R. B. (1971), Seismic anisotropy of the uppermost mantle absent beneath the east flank of the Reykjanes Ridge, *Bull. Seismol. Soc. Am.*, *61*, 1351–1368.